lubricants

MDPI

Article

Investigation of the Tribofilm Formation of HiPIMS Sputtered MoS_x Thin Films in Different Environments by Raman Scattering

Wolfgang Tillmann [1], Alexandra Wittig [1,*], Dominic Stangier [1], Carl-Arne Thomann [2], Henning Moldenhauer [2], Jörg Debus [2], Daniel Aurich [3] and Andreas Brümmer [3]

1 Institute of Materials Engineering, TU Dortmund University, Leonhard-Euler-Straße 2, 44227 Dortmund, Germany; wolfgang.tillmann@tu-dortmund.de (W.T.); dominic.stangier@tu-dortmund.de (D.S.)

2 Experimental Physics 2, TU Dortmund University, Otto-Hahn-Straße 4a, 44227 Dortmund, Germany; carlarne.thomann@tu-dortmund.de (C.-A.T.); henning.moldenhauer@tu-dortmund.de (H.M.); joerg.debus@tu-dortmund.de (J.D.)

3 Chair of Fluidics, TU Dortmund University, Leonhard-Euler-Straße 5, 44227 Dortmund, Germany; daniel.aurich@tu-dortmund.de (D.A.); andreas.bruemmer@tu-dortmund.de (A.B.)

* Correspondence: alexandra.wittig@tu-dortmund.de; Tel.: +49-231-755-4627

Received: 10 September 2019; Accepted: 5 November 2019; Published: 8 November 2019

Abstract: Understanding the generation of third body particles and their contribution to the formation of tribofilms of MoS_x thin films is still challenging due to a large number of influencing factors. Besides the structure of the as-deposited MoS_x films, the environment and the conditions during the Ball-on-disk tests affect tribofilms and thus the friction. Therefore, the influence of the surface pressure and sliding velocity in air, argon and nitrogen environments on the generation of the third body particles and the tribofilm formation of randomly oriented MoS_x films is investigated. A high surface pressure is one major factor to achieve low friction, especially under humid conditions, which is important considering the use in industrial applications, for example dry-running screw machines. However, the mechanisms leading to that frictional behavior are still affected by the surrounding environment. While low friction is caused by a more extensive tribofilm formation in air, in argon and nitrogen, large size third body particles dispensed all over the contact area contribute to a lower friction. Raman scattering reveal a different chemistry of these particles reflected in the absence of laser- or temperature-induced surface oxidation compared to the as-deposited film and the wear track. The Raman scattering results are discussed with respect to the wear particle size, its chemical reactivity and strain-induced bonding changes.

Keywords: MoS_x; third body particles; tribological behavior; surface pressure; sliding velocity; environment; Raman scattering

1. Introduction

Screw machines are rotary positive displacement machines that are used in various applications for gas compression. Due to the compact design and the low-maintenance operation, nowadays, screw machines are used in about half of all applications of compressed air supply and process gas technology [1]. Compared to common designs a dry-running unsynchronized screw machine has many advantages regarding the absence of synchronization gears, lubricants and peripheral devices [2]. To ensure the durability of the screw machine, a coating which resists the high forces and sliding velocities in the rotor contact is crucial. MoS_2 thin films show great potential to reduce the friction in the contact area of the rotors due to their structure and the ability of forming a tribofilm.

However, these properties strongly depend on the environmental conditions, whereby low friction can be achieved especially under inert conditions [3]. A degradation of the properties may be caused by an adsorption of water onto the surface and its diffusion into the film as well as an oxidation of the edge planes of MoS_2 [4]. Additionally, the (100) edge planes are favorite areas for water adsorption and, therefore, for limiting the crystallite alignment and the shearing of the planes [3]. Accordingly, the environmentally affected tribological properties can, in turn, be defined by changing the crystallite growth towards a strong (002) basal orientation [5]. Compared to that, in a nitrogen environment the reactive edge sites are saturated, because nitrogen reveals a high self-absorption tendency and can thus prevent an oxidation [6].

Considering the applications of MoS_x (where x is related to a non-stoichiometric composition) films on screw machines, the tribological properties of the MoS_x films must be provided over a wide range of sliding velocities and surface pressures. Similar to polymers and DLC films, MoS_x thin films show a surface pressure dependent friction behavior, where the friction decreases with increasing applied surface pressure [7]. Meng et al. reported that at a low surface pressure a ploughing effect of the asperities on the surface occurs. As the applied surface pressure increases, the asperities are gradually flattened, which reduces the friction between the coating and counterpart at 350 °C. Furthermore, the fluidity of the film material is proportional to the applied surface pressure, resulting in an increasing amount of the MoS_x transfer film [8]. Besides the impact on the equilibrium particle size and a formation of transfer film, Pope et al. stated that the magnitude of the applied force affects the recrystallization process occurring during the sliding. A high contact pressure enlarges the degree of the basal plane orientation and, therefore, reduces the coefficient of friction. However, this process is inhibited after the exposure of the surface to a high humidity [9]. The influence of the sliding speed on the tribological performance is directly linked to the formation of the transfer film. A high sliding speed causes a high tangential stress which removes the wear debris at the counterpart and makes it difficult to form the transfer film and complicates the transfer film formation, thus leading to high wear and friction [10].

The understanding of the mechanisms of the induced structural changes in the MoS_x films is still rudimentary with respect to the variation of the sliding velocity or the surface pressure. Hence, the structural properties of MoS_x films after the tribological tests are analyzed by resonant Raman scattering and X-ray diffraction. In order to differentiate between environmental influences and effects caused by tribological parameters, the tribological tests were carried out in air as well as in argon and nitrogen environments.

2. Materials and Methods

2.1. Film Deposition

The MoS_x films were synthesized by using an unbalanced magnetron sputtering device CC800/9 Custom (CemeCon AG, Würselen, Germany). Prior to the deposition, the substrate material (case-hardened steel 16MnCr5) was grinded and polished, Ra = (3.1 ± 0.6) nm. The entire process consisted of a heating and etching sequence followed by the deposition. Two molybdenum disulfide targets (99.95% purity) working at an average cathode power of 3 kW in HiPIMS mode were employed. A bias voltage of −100 V and a heating power of 1 kW (~125 °C) were applied. The pulse frequency was set to 1000 Hz and the pulse duration to 200 µs.

2.2. Film Characterization

The morphology and topography before and after a tribological test were analyzed by a field-emission scanning electron microscope (SEM) FE-JSEM 7001 (Jeol, Tokyo, Japan). The composition of the films was characterized by energy dispersive X-ray spectroscopy (EDS). X-ray diffraction (XRD) was used to investigate the crystallographic orientation of the MoS_x films. The XRD pattern was recorded using a diffractometer Advance D8 (Bruker, Madison, WI, USA) equipped with a Cr-Kα

radiation source (λ = 2.291 Å) in Bragg–Brentano configuration. The 2θ range was set from 10° to 100° with a step size of 0.035° and an exposure time of 1 s per step was applied. In addition, the phase specific residual stress of the hexagonal MoS_2 (100) and (110) reflexes were measured using the $\sin^2\psi$ method. The measurements were carried out in a 2θ range of 46° to 54° and 89° to 96°, respectively, with a step size of Δθ = 0.1° and an exposure time of 2.5 s. In order to identify possible anisotropic residual stresses, the rotation angle φ was selected for 0°, 45°, 90°, 135°, 180°, 225° and 270° and the tilt angle ψ was varied ensuring constant step size of $\sin^2\psi = 0.05$ in a range from 0° to 0.5°. To calculate the residual stress a Pearson fit was selected, using the elastic constants $s_1 = -2.404 \times 10^{-6}$ and $1/2\ s_2 = 2.163 \times 10^{-5}$. Regarding the mechanical properties, the hardness and the elastic modulus were determined by using the nanoindenter G200 (Agilent Technology, Santa Clara, CA, USA). In total 49 indents were established with a Berkovich diamond tip in continuous stiffness mode according to Oliver and Pharr [11]. For Raman scattering measurements, a confocal Raman microscope MonoVista CRS+ (S&I GmbH, Warstein, Germany) was used. This setup worked with a 633 nm continuous-wave HeNe laser, which was focused through a 20× objective UPLFLN20x (Olympus Corp., Tokyo, Japan.) on the film. The laser spot diameter was approximately 2 µm. The scattered light was analyzed by a spectrometer Acton Spectra Pro SP-2750 (Princeton Instruments, Princeton, NJ, USA) with a 900 grooves/mm holographic grating and a liquid-nitrogen-cooled charge-coupled-device camera Pylon (Princeton Instruments). To avoid laser artifacts in the scattering spectra, the HeNe laser light emission was cleaned and suppressed by filters. The tribological properties of the film were investigated by ball-on-disk tribometer tests (CSM-Instruments, Peseux, Switzerland) at room temperature with 5000 rotations in air, argon or nitrogen environment. 100Cr6 balls with a hardness of (11.3 ± 0.2) GPa were used as counterbodies. To create a defined environment, a cupola with a gas connection was mounted above the contact zone. During the whole test the gas flow rate was set to 10 bar per s. In each atmosphere the surface pressure and the sliding velocity was varied. A surface pressure of 1.3, 6.4 and 12.7 N/mm^2 (sliding velocity of 40 cm/s) and a sliding velocity of 10, 20 and 40 cm/s (surface pressure of 6.4 N/mm^2) were selected. After the tribometer tests the three-dimensional Profilometer InfiniteFocus (Alicona, Raaba/Graz, Austria). was used to calculate the wear coefficient. Therefore, the wear volume was determined by focus variation measurements and was subsequently normalized.

3. Results and Discussion

3.1. Structural and Mechanical Properties of the As-Deposited MoS_x Film

To specify the influence of the external surface pressure and sliding velocity on the MoS_x films, the as-deposited MoS_x film is characterized. The morphology may be described as columnar and the topography exhibits a granular and needle-like structure, see Figure 1. In addition, the X-ray diffraction pattern of the as-deposited film is shown in Figure 2. The typical (002), (100) and (110) reflexes related to the structure of hexagonal MoS_2 are seen, whereas the (100) reflex is more pronounced than the (002) reflex indicating a random orientation according to Reference [11]. The MoS_x film moreover possesses a sub-stoichiometric composition with an S/Mo ratio of (1.65 ± 0.02) and a film thickness of (5.40 ± 0.03) µm. The hardness is (0.73 ± 0.06) GPa and the elastic modulus is (52.70 ± 4.20) GPa. These structural properties of MoS_x thin films are affected by the adatom mobility related to the kinetic energy and temperature during the deposition process. Due to the applied bias-voltage in combination with the substrate temperature, the v-shaped columnar structure results from the adatoms diffusing between the adjacent grains and a competitive growth process tanking place between the differently oriented crystals. At the same time this mechanism manifests itself in the crystallographic orientation, since the (100) edge plane is chemically more reactive compared to the inert (002) basal plane and thus the probability of adsorption on the (100) surface is higher. The applied bias-voltage enhances the formation of the (100) edge plane and leads to a re-sputtering of the sulfur given by in a reduced S/Mo ratio. Besides the crystallographic orientation, the deposition parameters affect the residual stress of

vacuum-deposited thin films as proven by Homberg et al. for MoS_2 [12]. Therefore, the phase-specific residual stress of the hexagonal MoS_2 (100) and (110) reflexes was measured. The measurement of the residual stresses showed values of (−132.2 ± 106.7) MPa for the (100) reflex and (−13.6 ± 13.3) MPa for the (110) reflex. Although using HiPIMS technology the deposited film reveals an almost stress free state. Moreover, the investigation of the biaxial stress state exhibits an isotropic residual stress state for the main stresses. As stated by David et al. residual stresses result from a competition between stress formation by implantation of film atoms below the film surface and stress relaxation by thermal spike excited processes [12,13]. Thus, on the one hand, the bombardment with high kinetic ions due to the applied bias-voltage and on the other hand, the heating power during the deposition process are superimposed mechanisms leading to a stress free state of the deposited MoS_x thin film. In addition, the effect can be attributed to the layered molecular structure with individual sheets of molybdenum and sulfur atoms, which prevents the build-up of stresses as within nitride films. Low compressive residual stresses for sputtered MoS_x thin film were also reported by Holmberg et al., comparing these findings to higher compressive stresses in TiN thin films [14].

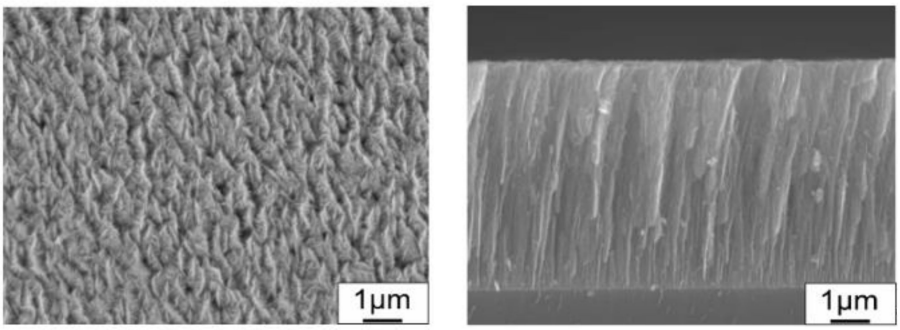

Figure 1. (**a**) Topography and (**b**) morphology of the as-deposited MoS_x film.

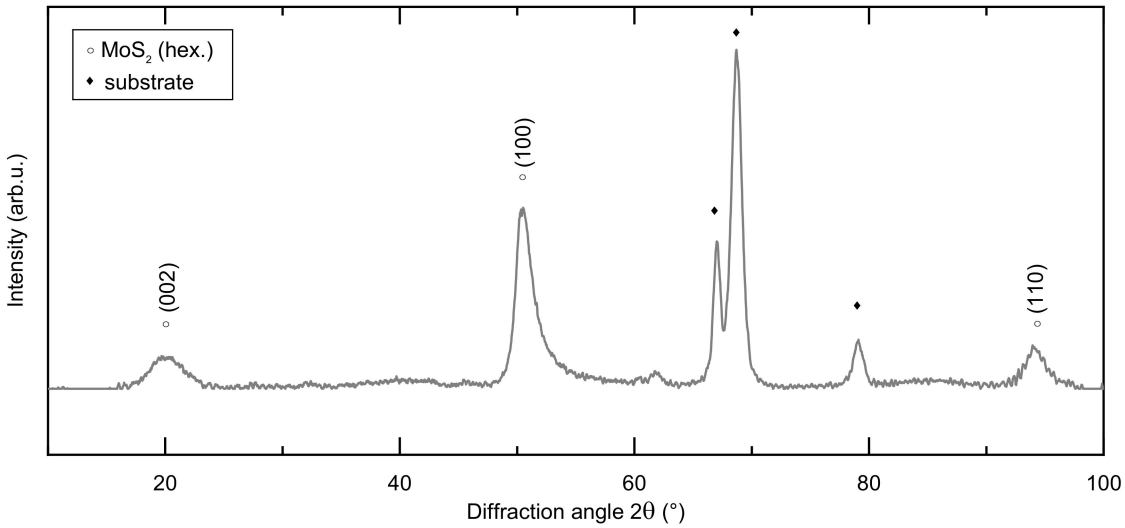

Figure 2. X-ray diffraction pattern of the as-deposited MoS_x film. The reflexes are attributed to either MoS_2 or the substrate.

Figure 3 shows the Raman spectrum of the as-deposited MoS_x film measured at a laser power of 0.18 mW. The spectrum contains optical phonon modes and out-of-plane (ZA) and in-plane longitudinal (LA) acoustic phonon modes which are typical for MoS_2 [15–18]. Within the frame of the point group D_{6h} notation, the most prominent optical phonon modes of MoS_2 are the E_{1g} mode at about 287 cm^{-1},

which describes an in-plane displacement of S atoms, the in-plane $E_{2g}{}^1$ mode at 372 cm^{-1} and the out-of-plane A_{1g} mode of only S atoms at 405 cm^{-1}. MoO_3 Raman peaks are not observed.

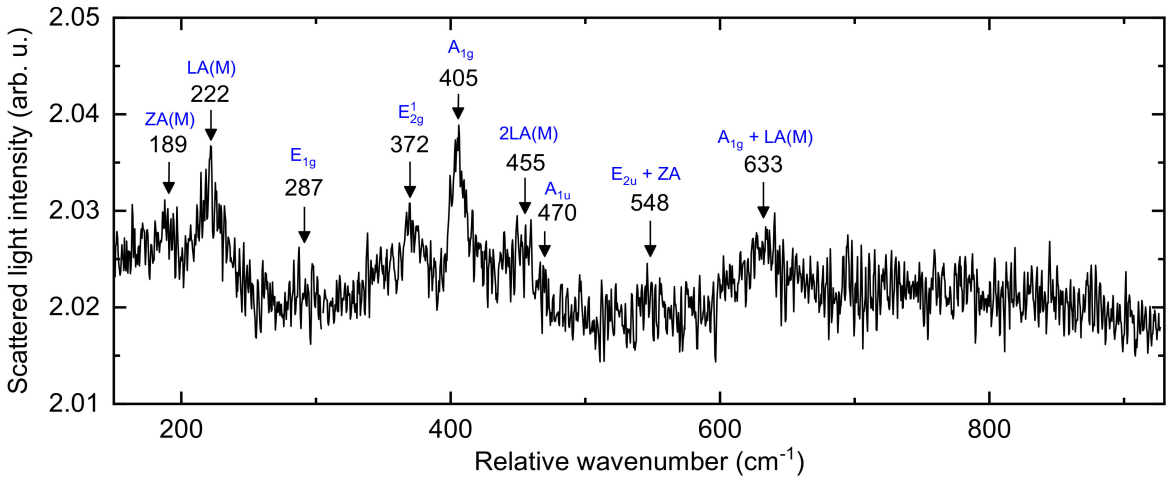

Figure 3. Raman spectrum of an as-deposited MoS_x film. The marked peaks stem from MoS_2.

3.2. Tribological Properties

The coefficients of friction of the MoS_x films against 100Cr6 counterparts as a function of the applied surface pressure and, respectively, the sliding velocity are depicted in Figure 4. The tribological tests carried out in air reveal a higher coefficient of friction independent of the applied surface pressure and the sliding velocity compared to the tests performed in argon or nitrogen. Furthermore, for the argon environment at high surface pressure and sliding velocity, μ is slightly lower compared to that obtained in a nitrogen environment. Apart from the differences in the absolute friction values, the functional dependence of μ on the applied surface pressure or the sliding velocity is similar for all three environments. The sliding velocity only weakly affects the friction, whereas the coefficient of friction decreases significantly with an increasing surface pressure.

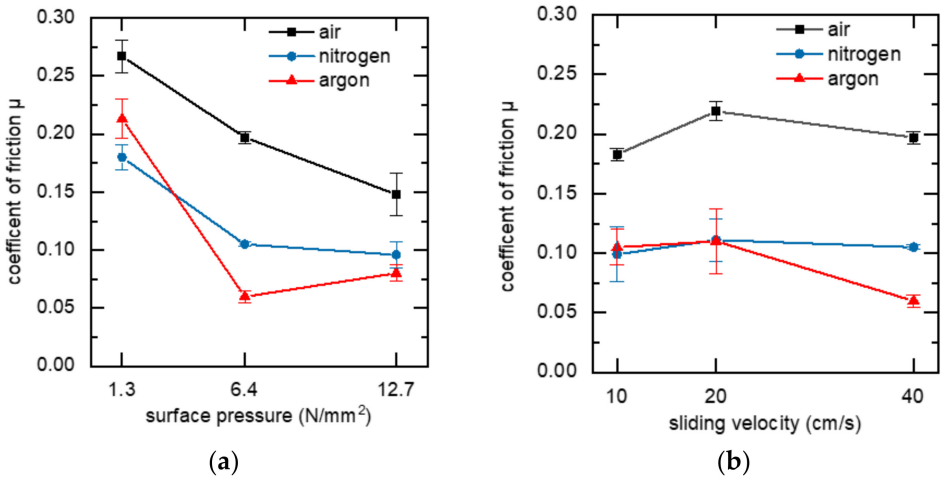

Figure 4. Coefficients of friction depending on the (**a**) surface pressure and (**b**) sliding velocity obtained in air (**squares**), nitrogen (**circles**) and argon (**triangles**) atmospheres.

The experimental results show the influence of the test environment on the friction behavior, which is related to the adsorption properties of MoS_x. The high friction in a humid environment is caused by the surrounding water molecules which are, for instance, responsible for limiting the crystallite alignment and shearing [3]. Since the investigated film is randomly oriented and the (100) crystallite edges are postulated to be favorite areas for water adsorption, the friction increases [19].

This mechanism is also related to the columnar crystallite growth; therefore, a bigger surface is exposed to the surrounding environment because common columnar coatings show a space of about 100 Å between the crystallites [5]. Thus, this structure allows moisture to penetrate easily into the coatings [20]. In addition, Holinski et al. reported that friction increases in presence of water due to the polar bonding between sulfur and water itself, which augmented the shear strength of the material [21]. Therefore, Matsumoto et al. reported a better humidity resistance for Mo-rich films [22], which should be considered since the investigated MoS_x thin film is sub-stoichiometric. Nitrogen, in contrast, adsorbs itself more easily than H_2O and occupies all available oxidization sites, which explains the absence of chemical segregation and the reduction in friction [23]. Increasing the sliding velocity or the surface pressure leads to a higher temperature in the contact area. It affects the surrounding water molecules: The chemisorbed water on the surface edge planes desorbs [24]. Due to that mechanism the friction should decrease at a high surface pressure or a high sliding velocity in a humid environment, which is important for the usage of an MoS_x film as solid lubricant on screw machines. This behavior is observed at a high surface pressure of about 12 N/mm^2. No or little changes regarding the friction values are seen at high velocities. Moreover, the water molecules and/or oxygen atoms are not solely responsible for the friction behavior observed, as water-free argon and nitrogen environments reveal a similar frictional behavior.

High temperatures may also promote oxidation processes, which primarily occur at the edge planes of the MoS_x surface [25]. Because the coefficient of friction does not increase, we conclude that the flash temperatures resulting from the sliding velocity or surface pressure are too low to initiate oxidation and, in turn, the formation of MoO_3. Khare et al. reported that even during a sliding process at 250 °C in air the oxidation does not have an adverse effect on the friction coefficient; in that context, it is stated that the oxidation rates may not compete with the rates of removing the film [4]. To confirm this assumption, the surfaces of the MoS_x films after the tribological tests are studied by Raman scattering spectroscopy which allows for identifying the chemical composition, oxidation as well as tribological films. Moreover, varying the laser power changes locally the temperature of the film surface; temperatures of more than 400 °C can be achieved with the experimental setup used [26]. In Figure 5a, the Raman spectra measured at the wear tracks of the MoS_x films, which were tested in the air, nitrogen or argon atmosphere at 1.3 N/mm^2 surface pressure, are shown. The Raman signatures are similar to that of the as-deposited MoS_x film, compare Figure 2. Thus, during the ball-on-disk tests molybdenum trioxide was not formed. Instead, an oxidation is induced by illuminating a worn position of an MoS_x film with high laser power (5.7 mW), see Figure 5b; MoO_3-related Raman modes at 290 and 810 cm^{-1} are observed. Additionally, the background at about 800 cm^{-1} is increased, which is probably due to the presence of further molybdenum-oxygen stretching modes [27].

The Raman spectra measured at worn surface areas, which were covered by debris, are depicted in Figure 5c for different environmental conditions and pressure parameters. The overall intensity of the scattering lines is enhanced for the MoS_x films tested in air, in contrast to the low-intensity-spectra of the films that were tested in the nitrogen and argon atmospheres. The Raman signatures are mostly related to MoS_2 phonon modes; their frequencies practically coincide with that obtained for the as-deposited film. For the MoS_x films tested, in particular, in argon and nitrogen atmosphere, quite significant Raman bands emerge at about 630, 750 and 845 cm^{-1}. While the first two bands may stem from second-order phonon scattering processes [28,29], the band at 845 cm^{-1} stems from Mo–N or Mo–C [29]. For these test conditions, we neglect the formation of molybdenum trioxide and, in turn, the observation of molybdenum-oxygen stretching modes in the Raman spectra. Furthermore, the Raman spectra from the debris areas of the worn MoS_x films, shown in Figure 5c, were measured at high laser power of 5.7 mW. Since MoO_3 Raman signals are not observed, we claim that an oxidation did not occur—even for a long-time laser illumination.

For the ball-on-disk experiments in N_2 and air atmospheres, in which the highest wear coefficients were measured, the wear of the MoS_x films leads to particles whose sizes are assumed to be in the range of at least several micrometers (larger than the exciting laser wavelength). For such sizes of particles,

also made from MoS_2, the chemical reactivity, in particular, the tendency of oxidation decreases, since the small surface areas of the particles limit the rate of oxidation [30,31]. Additionally, the scattering probability may become enlarged, while the probability of absorbing visible light and, in turn, inducing heat may be reduced. However, a surface-enhanced Raman scattering effect is negligible for these particle sizes. These two features may be characteristic of the tribological films formed during the wear tests. Both aspects explain the absence of laser- or, respectively, temperature-induced surface oxidation. The second aspect moreover provides a reason for the enhancement of the scattering intensity. Further studies shall provide insight into correlations between the formation of MoS_x debris, a potentially formed tribological film, thermal stability and the Raman scattering intensity.

We instead rule out a strain-induced intensity increase of the phonon lines due to the tribological tests. Strain typically causes a change in the bonding length and interaction strength between atoms, so that a frequency shift and/or a broadening of the phonon modes is more likely to occur. However, this is not the case. The residual stress caused by the growth technique of the MoS_x films can roughly be estimated from the frequencies of Raman scattering lines. An in-plane tensile strain, for MoS_2 nanosheets, results in shifts of the $E_{2g}{}^1$ and A_{1g} Raman lines to high frequencies [32]. According to Reference [32], the in-plane tensile strain in the HiPIMS MoS_x films may exceed 1%.

In Reference [33] it is proposed that weak disorder-induced lines, namely the acoustic phonon modes at around 200 cm^{-1}, may hint at a low coefficient of friction. In that context, the environmental conditions as well as the degree of wear and the formation of debris should be considered. Moreover, it seems that the wear tests in nitrogen atmosphere do not lead to an enhanced coverage of nitrogen atoms on the MoS_x surface. This would lead to an additional low-frequency shift of both the E_{12g} and A_{1g} phonon modes [34]. The sulfur atoms are more probably substituted by the nitrogen atoms giving rise to Mo-N Raman modes.

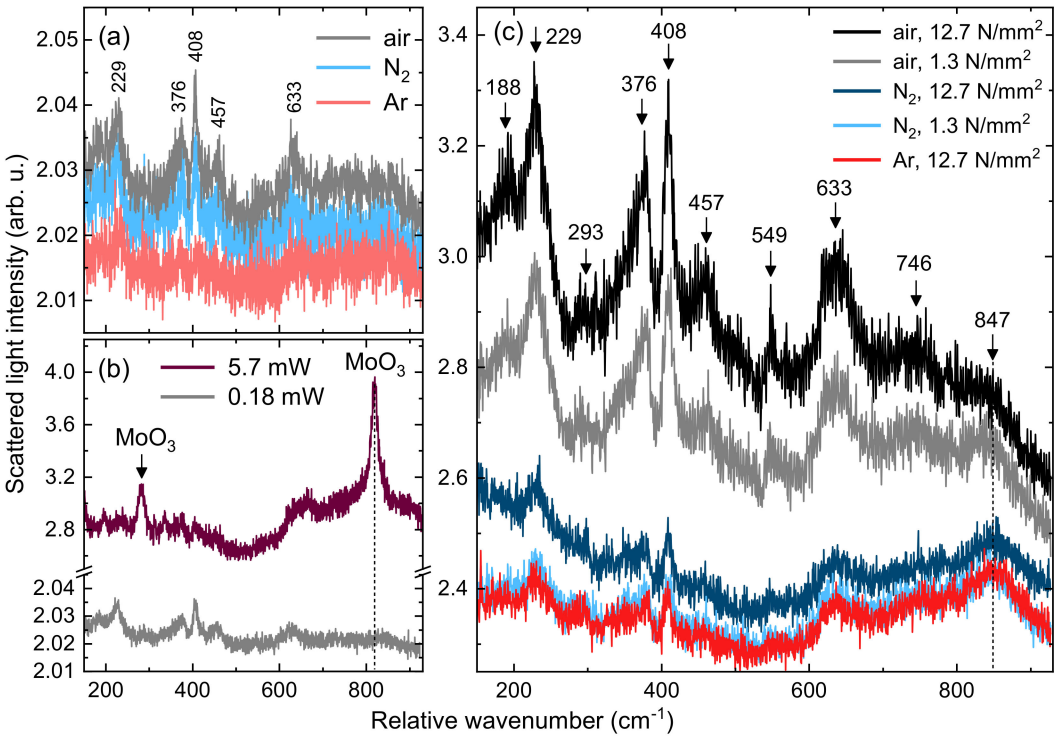

Figure 5. (**a**) Raman spectra of worn MoS_x measured at 0.18 mW laser power; surface pressure: 1.3 N/mm^2. (**b**) Raman spectra of worn MoS_x measured at two laser powers. (**c**) Raman spectra taken at debris of the worn MoS_x films; 5.7 mW laser power. The sliding velocity is 40 cm/s.

The crystallographic orientation of the worn surface or, respectively, the tribological film may differ from the as-deposited state of the MoS_x film [35,36]. To prove this point, X-ray diffraction

analyses were carried out after the tribological tests. The X-ray diffraction spectra of the as-deposited MoS_x film and exemplary wear tracks are illustrated in Figure 6. Compared to the crystallographic orientation of the as-deposited film, independent of the environment, the intensity of the (100) reflex decreases due to the sliding. The intensity of the (002) reflex is more pronounced after the tribological tests carried out in nitrogen atmosphere. Neither in air nor in nitrogen an increase of the surface pressure changes the reflex intensities. Since the well lubricating properties are ascribed to a (002) basal orientation [11], the higher intensity of this reflex and thus the shear planes after the tribological tests in nitrogen are assumed to be responsible for the low coefficient of friction.

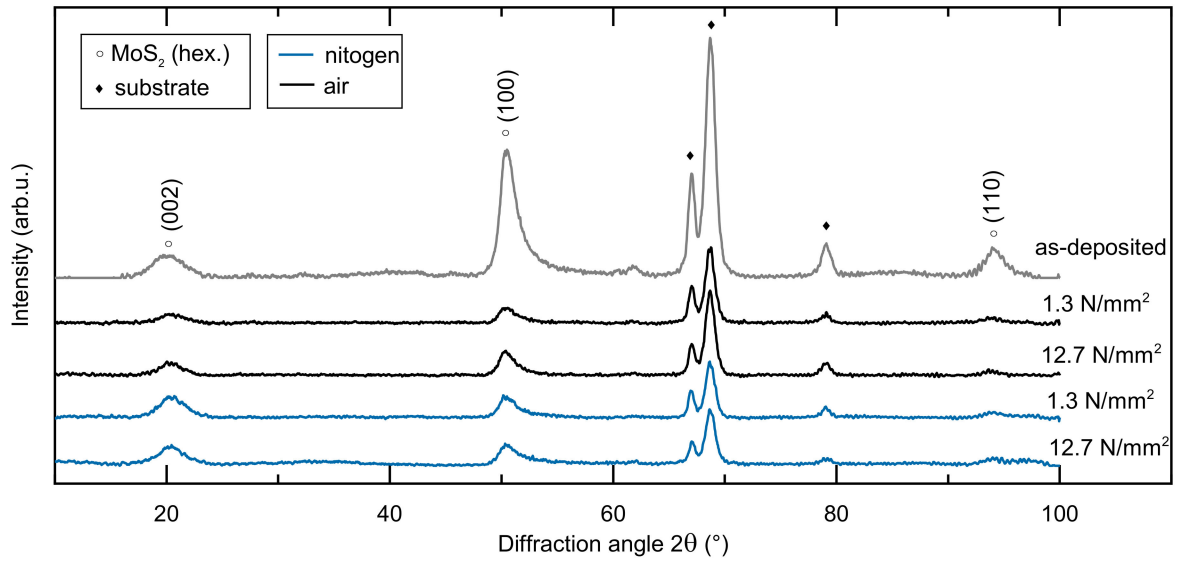

Figure 6. X-ray diffraction pattern of the as-deposited MoS_x film and exemplarily worn tracks. The reflexes are attributed to either MoS_2 or the substrate.

According to the model suggested by Singer et al., the detached material/debris on the surface trapped in the contact area may be beneficial for low friction, whereby the wear may be controlled by the loss flux of the depletion film material [37]. Considering the low hardness of the investigated MoS_x film and the removal of the film material under shear stress, material is detached from the surface with high probability. To investigate this effect, the wear coefficient was calculated and is illustrated in Figure 7. For each surface pressure and sliding velocity applied, the MoS_x films tested in air demonstrate the highest material removal. The trends of the wear coefficients in air are contrary to those in argon or nitrogen atmosphere. While the wear increases with an increasing surface pressure and sliding velocity in argon or nitrogen, it tends to decrease in air. As in the case of the coefficient of friction, the surface pressure more strongly impacts the tribological properties of the MoS_x film compared to the sliding velocity. This is also seen through the optical microscope of the Raman spectrometer system: MoS_x films worn in air and nitrogen atmospheres contain the highest amount of debris, while the ones tested in argon gas demonstrate only partially debris. This is also seen through the optical microscope of the Raman spectrometer system: MoS_x films worn in air and nitrogen atmospheres contain the highest amount of debris, while the ones tested in argon gas demonstrate only partially debris.

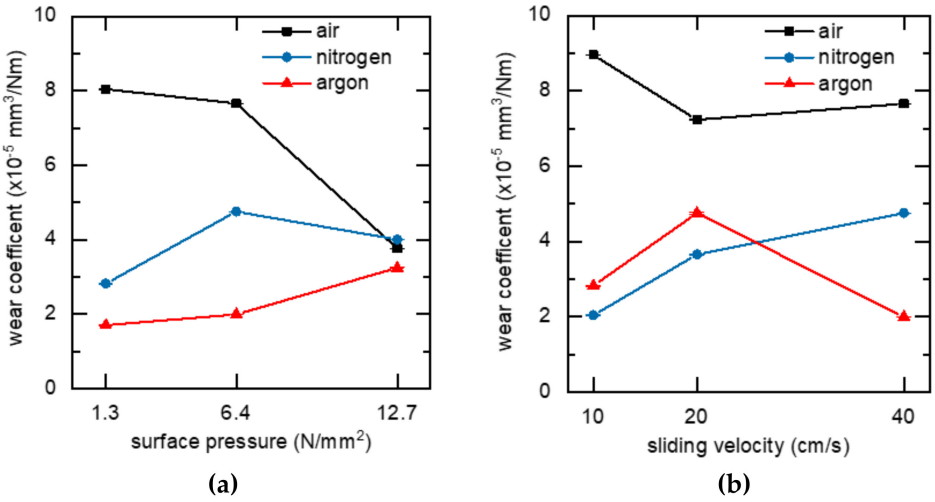

Figure 7. Wear coefficients depending on the (**a**) surface pressure and the (**b**) sliding velocity, for different environmental conditions during the ball-on-disk experiments.

To gain a further understanding of the processes occurring during the sliding and the wear mechanisms, scanning electron micrographs are taken after the tribological tests. Exemplary images are shown in Figure 8. All MoS_x films show grooves in sliding direction with the roughness asperities gradually flattened. At 1.3 N/mm^2 in a nitrogen environment, the MoS_x film covers the entire contact area. Increasing the surface pressure up to 12.7 N/mm^2 the film material is removed at local spots of the wear track leading to a wear particle agglomeration at the edge of the track and a substrate exposure. The film material is also completely removed in the contact area between the sample and the counterpart in air at a low surface pressure. The removal of the material may be reduced by an increased surface pressure, so that besides a local part the complete contact area is covered with MoS_x.

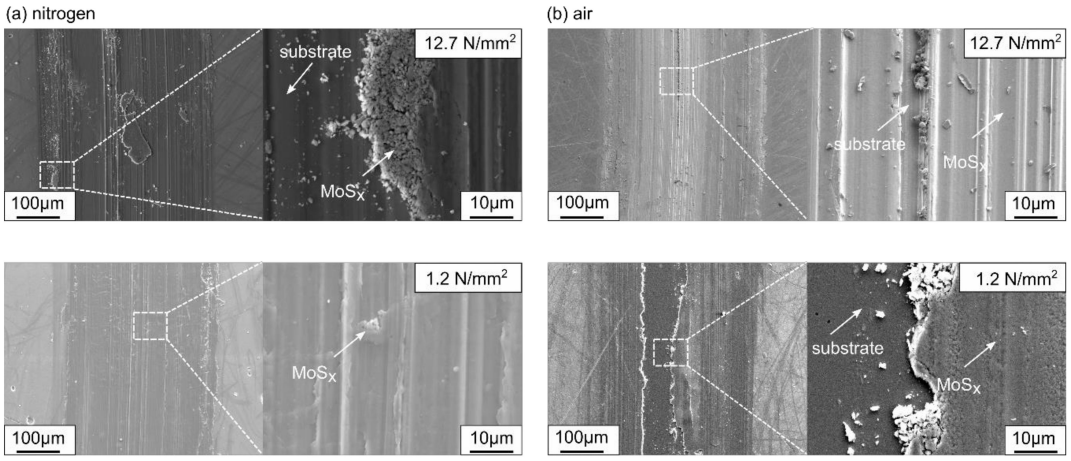

Figure 8. Scanning electron microscope images of the wear tracks of exemplary MoS_x films tested in (**a**) nitrogen and (**b**) air atmospheres, for different surface pressures.

After the tribometer tests in air at a low surface pressure, the MoS_x film is completely removed from the contact area, which explains the large coefficients of the wear and friction. However, the coefficient of friction is lower than that of a steel–steel contact suggesting that the wear particles are dragged along during the sliding and parts of them are transferred to the counterbody, which is also confirmed by the EDS analysis. Singer et al. reported that 2/3 of the film wears away during the running-in phase, because the columnar structure can break up in between the upper columns and their base. As the columns collapse, only the base region acts as a lubricating layer [38]. Therefore, it can be assumed that the upper part of the layer is removed and contributes to the formation of the wear particles, so that

the effective thickness of the lubricant is very limited. In contrast to that, the MoS_x film is dispensed all over the contact area in a nitrogen environment resulting in low wear and friction. Increasing the surface pressure leads to an enhanced fluidity of the film material [8] and a high temperature in the contact area. Due to that, the energy, which is necessary to break bonds and to form a wear particle, is reduced [24]. Thus, more wear particles will be generated at a high surface pressure or sliding velocity. Since these particles are responsible for the formation of the tribofilm, their creation does not inevitably result in a significant wear as long as they are not ejected from the contact area. In a nitrogen environment, the wear particles are sporadically within the contact area and the substrate material is only locally exposed; thus, the wear coefficient is slightly increased. This effect could be ascribed to the reorientation process already discussed within the scope of Figure 5, which indeed contributes to a low friction, but is responsible for a low interaction strength between the reoriented layer and the original film at the same time [6]. Compared to that, a high surface pressure or sliding velocity in air atmosphere gives rise to an improved tribofilm formation with a low amount of substrate material exposed which, in turn, yields a low wear and friction.

4. Conclusions

The influence of the surface pressure and sliding velocity on the generation of third body particles, the tribofilm formation and thus the tribological properties of MoS_x thin films in air, argon and nitrogen environments are studied. The coefficients of friction and wear of the MoS_x films tested in air atmosphere are higher than that in an argon or a nitrogen environment. These differences are ascribed to a mutual interaction between the adsorption behavior, the strength of the recrystallization process and the tribofilm formation. However, the trend of the friction and the wear due to an increasing surface pressure or sliding velocity is similar for all test environments. By increasing the surface pressure, more third body particles were generated, contributing to a thicker tribofilm and, thus, reduced friction and wear in air. Compared to that, in an argon or a nitrogen environment, large size third body particles are formed and dispensed all over the contact area. Even though the substrate is locally exposed and the wear rate increases due to that mechanism, the friction is reduced. Raman scattering spectroscopy reveals a different chemistry of these particles reflected by a decreased tendency of oxidation. Additionally, the scattering probability may become enlarged, while the probability of absorbing visible light may be reduced. To understand these characteristic features of the tribological films formed, in situ Raman scattering spectroscopy during the tribometer tests can provide further information about the correlations between the formation of MoS_x debris, a potentially formed tribological film, thermal stability and the Raman scattering intensity.

Author Contributions: Investigation, C.-A.T.; supervision, W.T., D.S., H.M., J.D., D.A. and A.B.; writing—review and editing, A.W.

Funding: This research received no external funding.

Acknowledgments: The authors acknowledge the German Research Foundation (DFG) for financially supporting this work within the priority program SPP2074 (Project "Fluid-free lubricant layers for the heavily loaded and unsynchronized operation of dry-running screw machines".

Conflicts of Interest: The authors declare no conflict of interest.

References

1. Hütker, J.; Brümmer, A. Physics of a dry running unsynchronized twin screw expander. In Proceedings of the 8th International Conference on Compressors and Their Systems, London, UK, 9–10 September 2013; Elsevier: Amsterdam, The Netherlands, 2013; pp. 407–416.
2. Debus, J.; Schindler, J.J.; Waldkirch, P.; Goeke, S.; Brümmer, A.; Biermann, D.; Bayer, M. Indication of worn WC/C surface locations of a dry-running twin-screw rotor by the oxygen incorporation in tungsten-related Raman modes. *Appl. Phys. Lett.* **2016**, *109*, 171601. [CrossRef]
3. Gradt, T.; Schneider, T. Tribological Performance of MoS2 Coatings in Various Environments. *Lubricants* **2016**, *4*, 32. [CrossRef]

4. Khare, H.S.; Burris, D.L. The Effects of Environmental Water and Oxygen on the Temperature-Dependent Friction of Sputtered Molybdenum Disulfide. *Tribol. Lett.* **2013**, *52*, 485–493. [CrossRef]
5. Vierneusel, B.; Schneider, T.; Tremmel, S.; Wartzack, S.; Gradt, T. Humidity resistant MoS2 coatings deposited by unbalanced magnetron sputtering. *Surf. Coat. Technol.* **2013**, *235*, 97–107. [CrossRef]
6. Colas, G.; Saulot, A.; Bouscharain, N.; Godeau, C.; Michel, Y.; Berthier, Y. How far does contamination help dry lubrication efficiency? *Tribol. Int.* **2013**, *65*, 177–189. [CrossRef]
7. Singer, I.L.; Bolster, R.N.; Wegand, J.; Fayeulle, S.; Stupp, B.C. Hertzian stress contribution to low friction behavior of thin MoS2 coatings. *Appl. Physic. Lett.* **1990**, *57*, 995–997. [CrossRef]
8. Meng, F.; Yang, C.; Han, H. Study on tribological performances of MoS2 coating at high temperature. *J. Eng. Tribol.* **2017**, *232*, 964–973. [CrossRef]
9. Pope, L.E.; Panitz, J. The effects of Hertzian Stress and Test Atmosphere on the friction coefficients of MoS2 coatings. *Surf. Coat. Technol.* **1988**, *36*, 341–350. [CrossRef]
10. Zhu, X.; Lauwerens, W.; Cosemans, P.; Van Stappen, M.; Celis, J.; Stals, L.; He, J. Different tribological behavior of MoS2 coatings under fretting and pinon-disk conditions. *Surf. Coat. Technol.* **2003**, *163*, 422–428. [CrossRef]
11. Fleischauer, P. Fundamental aspects of the electronic structure, materials properties and lubrication performance of sputtered MoS2 films. *Thin Solid Film* **1987**, *154*, 309–322. [CrossRef]
12. Windischmann, H. Intrinsic stress in sputter-deposited thin films. *Crit. Rev. Solid State Mater. Sci.* **1992**, *17*, 547–596. [CrossRef]
13. Davis, C.A. A simple model for the formation of compressive stress in thin films by ion bombardment. *Thin Solid Films* **1993**, *226*, 30–34. [CrossRef]
14. Holmberg, K.; Ronkainen, H.; Laukkanen, A.; Wallin, K.; Hogmark, S.; Jacobson, S.; Wiklund, U.; Souza, R.M.; Ståhle, P. Residual stresses in TiN, DLC and MoS2 coated surfaces with regard to their tribological fracture behaviour. *Wear* **2009**, *267*, 2142–2156. [CrossRef]
15. Wieting, T.J. Long-Wavelength lattice vibrations of MoS2 and GaSe. *Solid State Commun.* **1973**, *12*, 931–935. [CrossRef]
16. Mignuzzi, S.; Pollard, A.J.; Bonini, N.; Brennan, B.; Gilmore, I.S.; Pimenta, M.A.; Richards, D.; Roy, D. Effect of disorder on Raman scattering of single-layer MoS2. *Phys. Rev. B* **2015**, *91*. [CrossRef]
17. Stacy, A.M.; Hodul, D.T. Raman spectra of IVB and VIB transition metal disulfides using laser energies near the absorption edges. *J. Phys. Chem. Solids* **1985**, *46*, 405–409. [CrossRef]
18. Moldenhauer, H. Resonant Raman Scattering Characterizes Thermally Annealed HiPIMS Deposited. *Surf. Coat. Technol.* **2019**, *377*, 124891. [CrossRef]
19. Chen, Z.; He, X.; Xiao, C.; Kim, S. Effect of Humidity on Friction and Wear—A Critical Review. *Lubricants* **2018**, *6*, 74. [CrossRef]
20. Zhang, X. Effect of crystallographic orientation on fretting wear behaviour of MoS coatings in dry and humid air. *Thin Solid Film* **2001**, *396*, 69–77. [CrossRef]
21. Holinski, R.; Gänsheimer, J. A study of the lubricating mechanism of molybdenum disulfide. *Wear* **1972**, *19*, 329–342. [CrossRef]
22. Matsumoto, K. Tribological Performance of Sputtered MoS2 Films in Various Environment—Influence of oxygen concentration, water vapor and gas species. In Proceedings of the 8th European Space Mechanisms & Tribology Symposium, ESA SP-438, Toulouse, France, 29 September–1 October 1999.
23. Colas, G.; Saulot, A.; Regis, E.; Berthier, Y. Investigation of crystalline and amorphous MoS2 based coatings: Towards developing new coatings for space applications. *Wear* **2015**, *330*, 448–460. [CrossRef]
24. Colbert, R.S.; Sawyer, W.G. Thermal dependence of the wear of molybdenum disulphide coatings. *Wear* **2010**, *269*, 719–723. [CrossRef]
25. Khare, H.S.; Burris, D.L. Surface and Subsurface Contributions of Oxidation and Moisture to Room Temperature Friction of Molybdenum Disulfide. *Tribol. Lett.* **2013**, *53*, 329–336. [CrossRef]
26. Moldenhauer, H.; Bayer, M.; Debus, J.; Nikolov, A.; Brümmer, A. Raman scattering study of micrometer-sized spots of magnetite and hematite formed at 18CrNiMo7-6 screw rotor surfaces due to liquid-free, unsynchronized operation. *IOP Conf. Ser. Mater. Sci. Eng.* **2018**, *425*, 12016. [CrossRef]
27. Mo, T.; Xu, J.; Yang, Y.; Li, Y. Effect of carburization protocols on molybdenum carbide synthesis and study on its performance in CO hydrogenation. *Catal. Today* **2016**, *261*, 101–115. [CrossRef]

28. Chen, J.M.; Wang, C.S. Second order Raman spectrum of MoS2. *Solid State Commun.* **1974**, *14*, 857–860. [CrossRef]
29. Qiu, J. Formation of N-doped molybdenum carbide confined in hierarchical and hollow carbon nitride microspheres with enhanced sodium storage properties. *J. Mater. Chem.* **2016**, *4*, 13296–13306. [CrossRef]
30. Lavik, M.T.; Medved, T.M.; Moore, G.D. Oxidation characteristics of MoS2 and other solid lubricants. *ASLE Trans.* **1968**, *11*, 44–55. [CrossRef]
31. Liu, Y.; Yang, F.; Zhang, Y.; Xiao, J.; Yu, L.; Liu, Q.; Ning, Y.; Zhou, Z.; Chen, H.; Huang, W.; et al. Enhanced oxidation resistance of active nanostructures via dynamic size effect. *Nat. Commun.* **2017**, *8*, 14459. [CrossRef]
32. Yang, L.; Cui, X.; Zhang, J.; Wang, K.; Shen, M.; Zeng, S.; Dayeh, S.A.; Feng, L.; Xiang, B. Lattice strain effects on the optical properties of MoS2 nanosheets. *Sci. Rep.* **2014**, *4*, 5649. [CrossRef]
33. Tillmann, W.; Kokalj, D.; Stangier, D. Influence of the deposition parameters on the texture and mechanical properties of magnetron sputterd cubic MoNx thin films. *Materialia* **2018**, *5*, 100186. [CrossRef]
34. Qian, Q.; Zhang, Z.; Chen, K.J. In Situ Resonant Raman Spectroscopy to Monitor the Surface Functionalization of MoS2 and WSe2 for High-k Integration: A First-Principles Study. *Langmuir* **2018**, *34*, 2882–2889. [CrossRef] [PubMed]
35. Zhang, X.; Lauwerens, W.; He, J.; Celis, J.-P. Reorientation of randomly oriented MoSx coatings during fretting wear tests. *Tribol. Lett.* **2004**, *17*, 607–612. [CrossRef]
36. Fleischauer, P. Effects of Crystallite Orientation on Environmental Stability and Lubrication Properties of SputteredMoS2 Thin Films. *ASLE Trans.* **2008**, *27*, 82–88. [CrossRef]
37. Singer, I.L. Role of third bodies in friction and wear of protective coatings. *J. Vac. Sci. Technol.* **2003**, *A21*, 232–241. [CrossRef]
38. Singer, I.L.; Fayeulle, S.; Ehni, P.D. Wear behavior of triode-sputtered MoS 2 coatings in dry sliding contact with steel and ceramics. *Wear* **1996**, *195*, 7–20. [CrossRef]